Analysis of a short beam with application to solder joints: increased stand-off height relieves stress

E. Suhir,
Bell Laboratories, Basic Research, Murray Hill, NJ; Portland State University, Portland, OR, USA; Technical University, Vienna, Austria; Ariel University, Ariel, Israel, and ERS Co,
727 Alvina Ct., Los Altos CA 94024, USA, tel. 650-969-1530, suhire@aol.com

ABSTRACT

Physically meaningful and easy-to-use analytical (mathematical) stress model is developed for a short clamed-clamped beam with offset ends. The offset is assumed to be known in advance and is appreciably smaller than the beam's length (height) and even its thickness. The analysis is limited to elastic deformations. While the classical Timoshenko short-beam theory seeks the beam's deflection caused by the combined bending and shear deformations for the given loading, an inverse problem is considered here: the lateral force is sought for the given end displacement (offset). In short beams this force is larger than in long beams, since, in order to achieve the given displacement, the applied force has to overcome both bending and shear resistance of the beam.

It is envisioned that short beams could adequately mimic the state of stress in and the mechanical behavior of solder joint interconnections, including ball-grid-array (BGA) systems, characterized by large, compared to conventional joints, stand-off heights. When the package/printed-circuit-board (PCB) assembly is subjected to the change in temperature, the effective thermal expansion (contraction) mismatch of the package and the PCB materials results in the given (i.e., easily predictable) relative displacement (offset) of the ends of the solder joint. This offset can be easily determined beforehand from the known external thermal mismatch strain and the position of the joint with respect to the mid-cross-section of the assembly.

The maximum normal and shearing stresses could be viewed as suitable criteria of the beam's (joint's) material reliability. It is shown that these stresses can be brought down considerably by employing beam-like joints, i.e. joints with an increased stand-off height. It is imperative, of course, that, if such joints are employed, there is still enough interfacial real estate considered, so that the BGA bonding strength is not compromised. On the other hand, owing to the lower stress/strain level, assurance of the short and long-term reliability of a BGA system with elevated stand-off heights of the solder joints might be much less of a challenge than in the case of conventional joints. By employing beam-like solder joints one can even manage to avoid inelastic deformations of the joints, thereby increasing dramatically their lifetime.

Future work will include, but might not be limited to, the finite-element computations, experimental evaluations (such as, e.g., shear-off testing), and analyses of the occurrence and the role of the inelastic strains.

INTRODUCTION

Ball-grid-array (BGA) (Fig.1) is a widely used IC packaging technology [1-4]. It enables one to permanently surface mount electronic components on a printed circuit board (PCB) with high mounting density (high pin count). In addition, the application of the BGA technology leads to a short signal delay. The reliability of BGA solder joint interconnections is, however, a crucial bottleneck of the technology [5-12], especially if lead-free solder materials are considered [13-35]. The maximum normal and shearing stresses and strains often lead the BGA solder joints to fracture. These stresses could be viewed as suitable preliminary design-for-reliability criteria of the beam's material reliability.

One important disadvantage of the current BGA technology, as far as the induced stresses and long-term reliability are concerned, is that the BGA solder balls are not mechanically compliant. They do not flex the way the longer leads of the previous generations of the second level (package to PCB) interconnections were and are unable therefore to effectively relieve stresses and strains in the joints. Accordingly, the objective of this paper is to show that higher mechanical flexibility of solder joint interconnections can be achieved by employing joints with large (compared to conventional joints) stand-off heights. It is noteworthy in this connection that, as has been shown earlier [36] in application to Bell-Labs Si-on-Si flip-chip multi-chip packaging technology (Fig.2), solder joints configured as "pancakes" (i.e. those with large ratios of their diameter to the height) exhibit higher stresses and strains than joints configured as "balls" (i.e. joints with lower aspect ratios).

To demonstrate and to quantify the effectiveness of joints configured as short beams, an analytical (mathematical) stress model is developed. The possible length (height)-to-thickness ratio of the short beams

considered is always lower than ten and could be even as small as one, and therefore the effect of the shear deformations has to be accounted for. As to the offset, it is assumed to be always small compared to the beam's length (height) and even to its thickness. The analysis is limited to the elastic deformations.

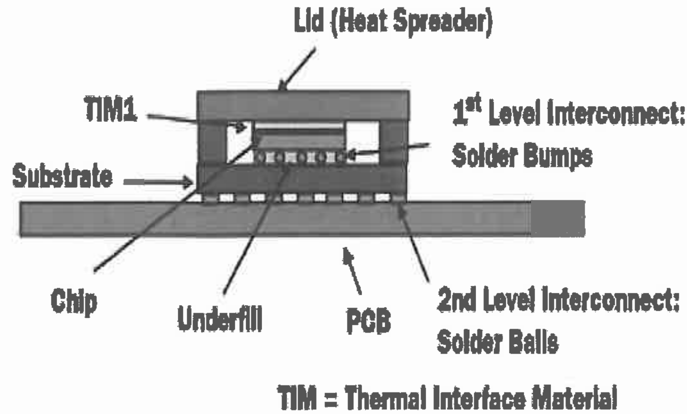

Fig.1. Ball Grid Array (BGA) technology

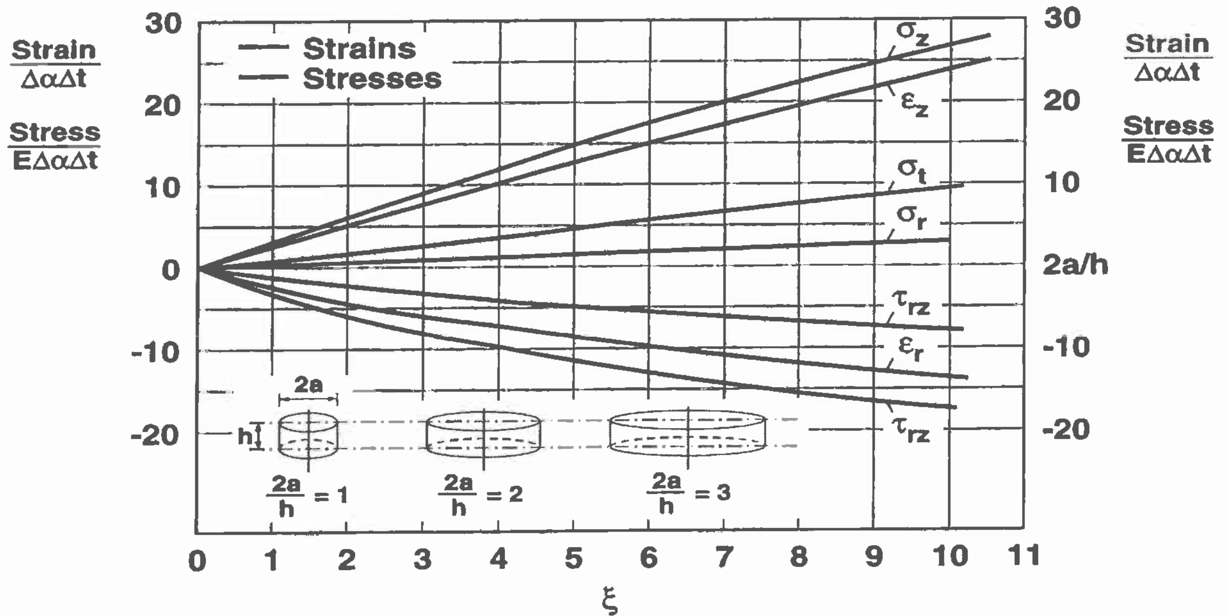

Fig.2. Thermal stresses and strains are higher for solder joint interconnections with higher ratio of their diameter to the standoff height.

Unlike the classical Timoshenko beam theory [37-39], when the total deflections caused by the combined bending and shear deformations are sought for the given loading, we consider an inverse problem: the lateral force is sought for the given total displacement (end offset). In a short beam, because of its deformation in shear, this force is expected to be larger than in a long beam, since such a shear force has to overcome both the bending and the shear resistance of the beam to achieve the given end offset.

ANALYSIS

Consider a short beam of unit width, length (height), h, and thickness $2l$. The beam's ends are clamped and are offset at the given distance Δ. The strain energy due to the beam's bending can be found as (see, e.g., [39])

$$V_b = \frac{1}{2EI}\int_0^h M^2(z)dz\,, \tag{1}$$

where EI is the beam's flexural rigidity, E is Young's modulus of the material, $I = \frac{2}{3}l^3$ is the moment of inertia of the beam's cross-section (per unit width), l is half the beam's thickness, h is its length (height),

$$M(z) = M_0\left(1 - \frac{2z}{h}\right) \tag{2}$$

is the (linearly) distributed bending moment,

$$M_0 = \frac{1}{2}N_0 h \tag{3}$$

are the bending moments at the clamped ends, and N_0 is the lateral force (this force does not change along the beam). The origin of the coordinate z is at the beam's lower end. The elastic curve $v(z)$ of the beam can be sought, in an approximate analysis, in the form of the method of initial parameters (see, e.g., [38]):

$$v(z) = \frac{M_0 z^2}{2EI} - \frac{N_0 z^3}{6EI} = \frac{N_0 z^2}{6EI}\left(\frac{3}{2}h - z\right)\,. \tag{4}$$

The condition $v(h) = \Delta$ yields:

$$M_0 = \frac{6\Delta EI}{h^2} = 4E\Delta\frac{l^3}{h^2}\,,\quad N_0 = \frac{12\Delta EI}{h^3} = 8E\Delta\left(\frac{l}{h}\right)^3\,, \tag{5}$$

and therefore the strain energy due to bending is

$$V_b = 4E\Delta^2\left(\frac{l}{h}\right)^3\,. \tag{6}$$

The strain energy due to shear (per unit volume and per unit beam's width) can be found as (see, e.g., [39]):

$$V_s'' = \frac{3(1+\nu)}{2E}\tau_{zx}^2\,, \tag{7}$$

where ν is Poisson's ratio of the material, and τ_{zx} is the shearing stress acting in the cross-sections of the beam and associated with the distortion of the beam's form. Assuming that this stress is distributed over the beam's cross-section in a parabolic fashion

$$\tau_{zx} = \tau_{\max}\left(1 - \frac{x^2}{l^2}\right), \tag{8}$$

we obtain the strain energy per unit beam length (height) by integrating this relationship over the beam's thickness:

$$V_s' = \frac{3(1+\nu)}{2E}\tau_{\max}^2 \int_{-l}^{l}\left(1-\frac{x^2}{l^2}\right)^2 dx = \frac{8}{5}\frac{1+\nu}{E} l\tau_{\max}^2 \quad . \tag{9}$$

In the formulas (8) and (9), $\tau_{\max}$ is the maximum shearing stress at the origin $(x = 0)$. From the obvious relationship

$$N_0 = \int_{-l}^{l}\tau_{zx}(x)dx = \tau_{\max}\int_{-l}^{l}\left(1-\frac{x^2}{l^2}\right)dx = \frac{4}{3}l\tau_{\max} \tag{10}$$

we have:

$$\tau_{\max} = \frac{3N_0}{4l} = 6E\Delta\frac{l^2}{h^3} \quad , \tag{11}$$

and the formula (9) yields:

$$V_s' = \frac{288}{5}(1+\nu)E\frac{\Delta^2 l^5}{h^6}. \tag{12}$$

For the entire beam the strain energy (per unit beam width) due to shear is

$$V_s = \frac{288}{5}(1+\nu)E\Delta^2\left(\frac{l}{h}\right)^6. \tag{13}$$

Equating the total strain energy

$$V = V_b + V_s = 4E\Delta^2\left(\frac{l}{h}\right)^3\left[1+\frac{72}{5}(1+\nu)\left(\frac{l}{h}\right)^3\right]. \tag{14}$$

to the work $W = \frac{1}{2}N\Delta$ of the external lateral force N, we obtain the following formula for this force:

$$N = 8E\Delta\left(\frac{l}{h}\right)^3\left[1+\frac{72}{5}(1+\nu)\left(\frac{l}{h}\right)^3\right] \quad . \tag{15}$$

Comparing this formula with the second formula in (5), we conclude that the lateral force N in the presence of shear deformations is larger by the factor of

$$\chi = 1+\frac{72}{5}(1+\nu)\left(\frac{l}{h}\right)^3 \tag{16}$$

than the force N_0 that does not consider these deformations. This is because the force N has to overcome not only bending, but also shear resistance of the beam in order to achieve the given offset of the beam's ends. The factor (16) changes from 1.0 (for very thin-and-tall beams characterized by the next-to-zero thickness-to-length (height) ratios), to 1.3, when this ratio is about 0.5 (for the Poisson's ratio of 0.33). From the relationships (11) and (15) we obtain the following formula for the maximum shearing stress

$$\tau_{\max} = 6E\frac{\Delta}{l}\left(\frac{l}{h}\right)^3\left[1+\frac{72}{5}(1+\nu)\left(\frac{l}{h}\right)^3\right]. \tag{17}$$

This formula indicates particularly that the maximum shearing stress decreases rapidly with the decrease in the ratio of the beam's length (height) to its thickness.

The normal stress

$$\sigma = \frac{3Nh}{4l^2} = \frac{h}{l}\tau_{\max} \tag{18}$$

in the beam, as long as a beam model is used, is always higher than the shearing stress.

It is noteworthy that in an opposite extreme case of a joint with a very low length (height)-to-thickness ratio, the maximum shearing stress can be sought, using the method of interfacial compliance [39], as

$$\tau_{\max} = \frac{\Delta}{\kappa},$$

where the interfacial compliance in the denominator can be found as the ratio of the vertical dimension (height) of the joint h to the shear modulus G of the material:

$$\kappa = \frac{h}{G}.$$

Thus, the maximum shearing stress is inversely proportional to the standoff height of the joint in the case of a plate-like joint and becomes inversely proportional to the cube of the standoff height in the case of a beam-like joint. The analysis of shearing and peeling stresses in an entire BGA assembly is provided in the Appendix. We would like to point out in this connection that the recent US Patent [40] that suggests using thicker masks will lead to larger stand-off heights of the BGA solder joints thereby resulting in lower induced stresses and in longer lifetime of the solder joints.

NUMERICAL EXAMPLE

Let, e.g., the CTE of the package and the PCB are $12x10^{-6}1/^0C$ and $18x10^{-6}1/^0C$, respectively, the change in temperature from the reflow soldering (fabrication) temperature to the room temperature is 275^0C, and the distance from the package mid-cross-section to the location of the given solder joint of the BGA system is $12.0mm$. The predicted thermally induced end offset of the solder joint is $\Delta = (18x10^{-6} - 12x10^{-6})x275x12 \approx 0.02mm$. Let the elastic constants of the solder material be $E = 30GPa = 3060kg/mm^2$ and $\nu = 0.30$, the height of the solder joint be $h = 0.8mm$, and half its thickness be $l = 0.2mm$. Then the formulas (17) and (18) yield: $\tau_{\max} = 37.1kg/mm^2$ and $\sigma = 148.3kg/mm^2$. If the stand-off height is made $h = 1.6mm$, then the predicted stresses are $\tau_{\max} = 3.7kg/mm^2$ and $\sigma = 29.7kg/mm^2$. The change is significant.

CONCLUSIONS

- Physically meaningful and easy-to-use analytical (mathematical) stress model is developed for a short beam with clamped and offset ends. Unlike the classical Timoshenko beam theory, when the total deflections caused by the combined bending and shear deformations are sought for the given loading, we consider an inverse problem and seek the lateral force that caused the given total displacement (ends offset). In a short beam, because of its deformation in shear, this force should be larger than in a long beam, since it has to overcome both the bending and the shear resistance of the beam to achieve the given end offset.
- The induced stresses in solder joints can be brought down considerably by employing beam-like joints. It is imperative, of course, that if such joints are employed for lower stresses, there is still enough interfacial real estate not to compromise the BGA bonding strength. On the other hand, owing to a lower stress level in BGA systems with elevated standoff heights, assurance of their strength might be much less of a challenge than in the case of conventional joints
- The maximum shearing stress is inversely proportional to the square root of the standoff height of the joint in the case of a plate-like (small standoff height) joint and is inversely proportional to the cube of the standoff height in the case of a beam-like (significant standoff height) joint.

- The maximum peeling stress is inversely proportional to the standoff height of the joint in the case of a plate-like (small standoff height) joint and is next-to-zero in the case of a beam-like (significant standoff height) joint.
- By employing beam-like solder joints one might even avoid inelastic deformations in them, thereby increasing dramatically the lifetime of the material.
- Future work will include, but might not be limited to, the finite-element computations, experimental evaluations (e.g., shear-off testing), as well as to the accounting for the effect of inelastic deformations, if any.

REFERENCES

1. J. Lau, "Ball Grid Array Technology", McGraw-Hill, 1994
2. J. Lau, C. Wong, J. Prince and W. Nakayama, "Electronic Packaging: Design, Materials, Process, and Reliability", McGraw-Hill, New York, 1998.
3. E. Suhir, CP Wong, YC Lee, eds. "Micro- and Opto-Electronic Materials and Structures: Physics, Mechanics, Design, Packaging, Reliability", 2 volumes, Springer, 2008
4. IPC-SM-782, Surface Mount Design and Land Pattern Standards, Section 8, 93. http://www.matweb.com . Accessed on July 15, 2008.
5. H.H. Manko, "Solders and Soldering: Materials, Design, Production and Analysis for Reliable Bonding", McGraw-Hill, 1979.
6. J.H.L. Pang, "Solder Joint Reliability: Theory and Applications", Van Nostrand Reinhold, 1991.
7. R. Darveaux and K. Banerji, "Constitutive Relations for Tin-Based Solder Joints", IEEE CHMT Transactions, vol. 15, No.6, 1992
8. Y.H. Pao, S. Badgley, R. Govila and E. Jih, "Experimental and Modeling Study of Thermal Cyclic Behavior of Sn-Cu and Sn-Pb Solder Joints", MRS Symposium Proceeding, vol. 323,1994, pp.153-158.
9. R. Darveaux, K. Banerji, A. Mawer and G. Dody. "Reliability of Plastic Ball Grid Array Assemblies. Ball Grid Array Technology", McGraw-Hill, 1995
10. J. Lau and Y. Pao, "Solder Joint Reliability of BGA, CSP, Flip Chip, and Fine Pitch SMT Assemblies", McGraw-Hill, New York, 1997.
11. Q. Yu, M. Shiratori and Y. Oshima, "Thermal Fatigue Reliability Assessment for Solder Joints of BGA Assembly", The 11th Computational Mechanics Conference, JSME, No. 98-2, 1998, pp. 507-508
12. Q.Yu and M. Shiratori, "Effects of BGA Solder Geometry on Fatigue Life and Reliability Assessment", JIEP Journal, Vol. 1, No. 4, 1998, pp. 278-283
13. Y. Kariya and W. J. Plumbridge, "Mechanical Properties of Sn3.0%Ag-0.5%Cu alloy, Proceedings, 7th Symp. on Microjoining and Assembly Technology in Electronics. Feb. 1-2, Yokohama, Japan, 2001, pp.383-388.
14. J. Lau, Z. Mei, S. Pang, C. Amsden, J. Rayner, and S. Pan, "Creep Analysis and Thermal-Fatigue Life Prediction of the Lead-Free Solder Sealing Ring of a Photonic Switch", ASME Transactions, Journal of Electronic Packaging, Vol. 124, December 2002, pp. 403-410.
15. C. B. Lee, S. B. Jung, Y. E. Shin, and C. C. Shur, "Effect of Isothermal Ageing on Ball Shear Strength in BGA Joints with Sn-3.5Ag-0.75Cu Solder," Materials Transactions, Vol. 43, No. 8, 2002, pp. 1858 – 1863
16. M. Painaik, and D. L. Santos, "Effect of Flux Quantity on Sn-Pb and Pb-Free BGA Solder Shear Strength", SEMI Technology Symposium: International Electronics Manufacturing Technology (IEMT) Symposium, 2002, pp. 229 -237
17. H.J.Song, J. W. Morris, and F. Hua, "The Creep Properties of Lead-Free Solder Joints", Journal of Materials, June 2002, pp. 30-32.
18. Q. Zhang, A. Dasgupta and P. Haswell. "Viscoplastic Constitutive Properties and Energy-Partitioning Model of Lead-Free Sn3.9Ag0.6Cu Solder Alloy", IEEE ECTC, 2003
19. J.Lau, W. Dauksher, and P. Vianco, "Acceleration Models, Constitutive Equations and Reliability of Lead-Free Solders and Joints", IEEE ECTC, 2003, pp. 229-236.
20. S. Wiese et al., "Microstructural Dependence of Constitutive Properties of Eutectic SnAg and SnAgCu Solders", IEEE ECTC, 2003, .pp.197-206.
21. A. Schubert, R. Dudek, E. Auerswald, A. Gollhardt, B. Michel and H. Reicbl. "Fatigue Life Models for SnAgCu and SnPb Solder Joints Evaluated by Experiments and Simulation", IEEE ECTC, 2003

22. A. Schubert, A., R. Dudek, E. Auerswald, A. Gollhardt, B. Michel, and H. Reichl, "Fatigue Life Models for SnAgCu and SnPb Solder Joints Evaluated by Experiments and Simulation", IEEE ECTC, 2003, pp. 603-610.
23. J. Lau, W. Dauksher and P. Vianco "Acceleration Models, Constitutive Equations and Reliability of Lead-free Solders and Joints" .Proceeding IEEE ECTC, 2003, pp.229-236.
24. A. R. Syed, "Accumulated Creep Strain and Energy Density Based Thermal Fatigue Life Prediction Models for SnAgCu Solder Joints", IEEE ECTC, 2004, pp.737-746.
25. Q. Xiao, L. Nguyen, W. D. Armstrong, "Aging and Creep Behavior of Sn3.9Ag0.6Cu Solder Alloy," IEEE ECTC, 2004, pp. 1325 – 1332
26. J. Lau, D. Shangguan, D. Lau, T. Kung, and R. Lee, "Thermal-Fatigue Life Prediction Equation for Wafer-Level Chip Scale Package (WLCSP): LeadFree Solder Joints on Lead-Free Printed Circuit Board (PCB)", IEEE ECTC, 2004, pp. 1563-1569.
27. K. Newman, "BGA Brittle Fracture – Alternative Solder Joint Integrity Test Methods," IEEE ECTC, 2005, pp. 1194 – 1201
28. S. Ridout and C. Bailey, "Review of Methods to Predict Solder Joint Reliability Under Thermo-Mechanical Cycling". Fatigue Engng Mater Struct.30, 2006, pp.400-412.
29. M. Osterman and A. Dasgupta, "Life Expectancies of Pb-Free SAC Solder in-Terconnects in Electronic Hardware", J Master Sci. 18, 2007, pp.229-236.
30. B. Vandevelde, M. Gonzalez, P. Limaye, P. Ratchev and E. Beyne, "Thermal Cycling Reliability of SnAgCu and SnPb Solder Joints: A Comparison for Several IC-Packages", Microelectronics Reliability.47, 2007, pp.259-265.
31. M. Spraul, W. Nuchter, A. Moller, B. Wunderle and B. Michel, "Reliability of SnPb and Pb-free Flips Under Different Test Conditions", Microelectronics Reliability.47, 2007, pp.252-258.
32. J. M. Koo, and S. B. Jung, "Effect of Displacement Rate on Ball Shear Properties for Sn–37Pb and Sn–3.5Ag BGA Solder Joints During Isothermal Aging," Microelectronics Reliability, vol.47, 2007, pp.2169–2178
33. A.M. Lajimi, J. Cugnoni and J. Botsis, "Reliability Analysis of Lead-free Solders", Proceedings of the World Congress on Engineering and Computer Science 2008, WCECS 2008, San Francisco, USA, October 22 - 24, 2008,
34. ESA PSS 01-708 The Manual Soldering of High-Reliability Electrical Connections. Noordwijk Netherlands: ESA Publications Division.
35. ESA PSS 01-738 High-Reliability Soldering for Surface-Mount and Mixed Technology Printed-Circuit Boards. Noordwijk Netherlands: ESA Publications Division.
36. E. Suhir, "Axisymmetric Elastic Deformations of a Finite Circular Cylinder with Application to Low Temperature Strains and Stresses in Solder Joints", ASME J. Appl. Mech., vol. 56, No. 2, 1989.
37. S.P. Timoshenko, "On the Correction Factor for Shear of the Differential Equation for Transverse Vibrations of Bars of Uniform Cross-Section", Philosophical Magazine, 1921, p. 744.
38. S. P. Timoshenko, and J. M. Gere, "Mechanics of Materials". Van Nostrand Reinhold Co., 1972.
39. E. Suhir, "Structural Analysis in Microelectronic and Fiber Optic Systems, Basic principles of Engineering Elasticity and Fundamentals of Structural Analysis", van Nostrand Reinhold, New York, 1991.
40. A. Yaung and N.S.Greenberg, "Printed Circuit Board", US Patent 2007/0056765 A1, March 15, 2007

APPENDIX

Interfacial stresses in small standoff-height assemblies

The analysis that follows is carried out under an assumption that the stresses in and the performance of a long enough BGA can be evaluated by replacing, when carrying out predictive stress modeling, an actual BGA with a continuous layer of solder of the same standoff height as the actual BGA is. The interfacial longitudinal displacement can be sought, in an approximate analysis, using the interfacial compliance concept [39], in the form:

$$u_1(x) = -\alpha_1 \Delta t x + \lambda_1 \int_0^x N(\xi) d\xi - \kappa_1 \tau(x) - \frac{h_1}{2} w_1'(x),$$

$$u_2(x) = -\alpha_2 \Delta t x + \lambda_2 \int_0^x N(\xi) d\xi + \kappa_2 \tau(x) + \frac{h_2}{2} w_2'(x). \quad \text{(A-1)}$$

Here α_1 and α_2 ($\alpha_1 \prec \alpha_2$) are the effective coefficients of thermal extension (contraction) of the package and the PCB materials, Δt is the change in temperature from the fabrication temperature to the low (room or testing) temperature, $\lambda_1 = \frac{1-\nu_1}{E_1 h_1}$ and $\lambda_2 = \frac{1-\nu_2}{E_2 h_2}$ are the axial compliances of the PCB and the package materials, respectively, E_1, ν_1 and E_2, ν_2 are the elastic constants of the materials, h_1 and h_2 are the thicknesses of the PCB and the package,

$$N(x) = \int_{-L}^{x} \tau(\xi) d\xi \quad \text{(A-2)}$$

is the thermally induced force acting ion the cross-sections of the package and the PCB, L is half assembly length, $\tau(x)$ is the so far unknown interfacial shearing stress, $\kappa_1 = \frac{h_1}{3G_1}$ and $\kappa_2 = \frac{h_2}{3G_2}$ are the effective longitudinal interfacial compliances of the PCB and the package, $G_1 = \frac{E_1}{2(1+\nu_1)}$ and $G_2 = \frac{E_2}{2(1+\nu_2)}$ are the effective shear moduli of the PCB and the package materials, and $w_1(x)$ and $w_2(x)$ are the deflection functions of the PCB and the package. The origin of the coordinate x is in the mid-cross-section of the assembly. The condition of the displacement compatibility can be written as

$$u_1(x) - u_2(x) = \kappa_0 \tau(x), \quad \text{(A-3)}$$

where $\kappa_0 = \frac{h}{G}$ is the longitudinal interfacial compliance of the BGA (attachment) [39]. Substituting the equations (A-1) into this condition we obtain:

$$\kappa \tau(x) - (\lambda_1 + \lambda_2) \int_0^x N(\xi) d\xi + \frac{h_1}{2} w_1'(x) + \frac{h_2}{2} w_2'(x) = \Delta\alpha \Delta t x, \quad \text{(A-4)}$$

where $\kappa = \kappa_0 + \kappa_1 + \kappa_2$ is the total longitudinal interfacial compliance of the assembly, and $\Delta\alpha = \alpha_1 - \alpha_2$ is the CTE difference between the PCB and the package.

Differentiating the equation (A-4) with respect to the coordinate x we have:

$$\kappa \tau'(x) - (\lambda_1 + \lambda_2) N(x) + \frac{h_1}{2} w_1''(x) + \frac{h_2}{2} w_2''(x) = \Delta\alpha \Delta t \quad \text{(A-5)}$$

Since no concentrated longitudinal external forces act at the assembly ends, the boundary condition $N(\pm L) = 0$ should be fulfilled, and since no concentrated bending moments act at the assembly ends, the conditions $w_1''(\pm L) = 0$ and $w_2''(\pm L) = 0$ for the curvatures should be fulfilled. Then the equation (A-5) results in the following condition for the shearing stress function $\tau(x)$:

$$\tau(\pm L) = \pm \frac{\Delta\alpha \Delta t}{\kappa} \quad . \quad \text{(A-6)}$$

Treating the PCB and the package as rectangular plates, we have the following equation of their bending (equilibrium):

$$D_1 w_1''(x) = -\frac{h_1}{2} N(x) - \int_{-L}^{x} \int_{-L}^{x} p(\xi) d\xi d\xi_1, \quad D_2 w_2''(x) = -\frac{h_2}{2} N(x) + \int_{-L}^{x} \int_{-L}^{x} p(\xi) d\xi d\xi_1. \quad \text{(A-7)}$$

Here $D_1 = \frac{E_1 h_1^3}{12(1-\nu_1^2)}$ and $D_2 = \frac{E_2 h_2^3}{12(1-\nu_2^2)}$ are flexural rigidities of the PCB and the package, and $p(x)$ is the peeling stress. The PCB and the package curvatures are therefore

$$w_1''(x) = -\frac{h_1}{2D_1}N(x) - \frac{1}{D_1}\int_{-L}^{x}\int_{-L}^{x} p(\xi)d\xi d\xi_1, \quad w_2''(x) = -\frac{h_2}{2D_2}N(x) - \frac{1}{D_2}\int_{-L}^{x}\int_{-L}^{x} p(\xi)d\xi d\xi_1 \quad \text{(A-8)}$$

Note that since the force $N(x)$ and the moment $\int_{-L}^{x}\int_{-L}^{x} p(\xi)d\xi d\xi_1$ are zero at the assembly ends, the curvatures (A-8) are zero as well.

Introducing the formulas (A-8) into the equation (A-5) we obtain the following equation for the interfacial shearing stress function $\tau(x)$:

$$\kappa\tau'(x) - \lambda N(x) + \mu\int_{-L}^{x}\int_{-L}^{x} p(\xi)d\xi d\xi_1 = \Delta\alpha\Delta t \,. \quad \text{(A-9)}$$

Here

$$\lambda = \lambda_1 + \lambda_2 + \frac{h_1^2}{4D_1} + \frac{h_2^2}{4D_2} \quad \text{(A-10)}$$

is the axial compliance of the assembly with consideration of its finite flexural rigidity (with consideration of bending), and

$$\mu = \frac{h_1}{2D_1} - \frac{h_2}{2D_2} \quad \text{(A-11)}$$

is the parameter that considers the difference in the flexural rigidities of the PCB and the package. The formula (A-10) indicates that finite flexural rigidities of the PCB and the package result in higher axial compliance of the assembly and, hence, in higher values of the parameter of the interfacial shearing stress (see formula (A-14) below). In an approximate analysis, aimed at the assessment of the role of the BGA compliance, the parameter μ can be put equal to zero, so that the shearing and the peeling stresses are not coupled. Then the shearing stress can be evaluated from the simplified equation:

$$\kappa\tau'(x) - \lambda N(x) = \Delta\alpha\Delta t \quad \text{(A-12)}$$

Considering (A-2), this equation results in the following equation for the induced force $N(x)$:

$$N''(x) - k^2 N(x) = \frac{\Delta\alpha\Delta t}{\kappa}, \quad \text{(A-13)}$$

where

$$k = \sqrt{\frac{\lambda}{\kappa}} \quad \text{(A-14)}$$

is the parameter of the interfacial shearing stress.

We seek the solution to the equation (A-13) in the form:

$$N(x) = C_0 + C_2 \cosh kx \,. \quad \text{(A-15)}$$

Since the condition $N(\pm L) = 0$ has to be fulfilled, the solution (A-15) yields: $C_2 = -\frac{C_0}{\cosh kL}$, and can be written as $N(x) = C_0\left(1 - \frac{\cosh kx}{\cosh kL}\right)$. Introducing this formula into the equation (A-13), we obtain: $C_0 = -\frac{\Delta\alpha\Delta t}{\lambda}$. Thus, the solution (A-15) results in the following expression for the lateral force:

$$N(x) = -\frac{\Delta\alpha\Delta t}{\lambda}\left(1 - \frac{\cosh kx}{\cosh kL}\right). \tag{A-16}$$

The interfacial shearing stress can be found, as follows from the formula (A-2), by differentiation:

$$\tau(x) = N'(x) = k\frac{\Delta\alpha\Delta t}{\lambda}\frac{\sinh kx}{\cosh kL}. \tag{A-17}$$

This solution meets the boundary condition (A-6).

For a long assembly (in the longitudinal direction), when $kL \geq 2.5$, the solution (A-17) can be written as

$$\tau(x) = k\frac{\Delta\alpha\Delta t}{\lambda}e^{-k(L-x)} = \tau_{\max}e^{-k(L-x)}, \tag{A-18}$$

where

$$\tau_{\max} = k\frac{\Delta\alpha\Delta t}{\lambda} = \frac{\Delta\alpha\Delta t}{\sqrt{\lambda\kappa}} \tag{A-19}$$

is the maximum value of the interfacial shearing stress. It takes place at the assembly ends and decreases exponentially with the increase in the distance of the given cross-section from the assembly ends.

Assuming that the PCB and the package are very rigid compared to the BGA system, so that the interfacial compliance of this system can be found as $\kappa \approx \kappa_0 = \frac{h}{G}$, we obtain the formula (A-19) in the following approximate form:

$$\tau_{\max} = \Delta\alpha\Delta t\sqrt{\frac{G}{\lambda h}} \quad . \tag{A-20}$$

Thus, the maximum interfacial shearing stress in a long enough assembly is assembly length independent and is inversely proportional to the square root of the BGA stand-off height.

For a short assembly (in the longitudinal direction), when $kL \leq 0.25$, the solution (A-17) yields

$$\tau(x) = \frac{\Delta\alpha\Delta t}{\kappa}x = \tau_{\max}\frac{x}{L}, \tag{A-21}$$

where the maximum value

$$\tau_{\max} = \frac{\Delta\alpha\Delta t}{\kappa}L \tag{A-22}$$

of the interfacial shearing stress takes place at the assembly ends. The interfacial shearing stress is linearly distributed along the assembly. Assuming that the PCB and the package are very rigid compared to the BGA system, so that the interfacial compliance of this system can be found as $\kappa \approx \kappa_0 = \frac{h}{G}$, we obtain the formula (A-22) in the following approximate form:

$$\tau_{\max} = G\frac{\Delta\alpha\Delta t}{h}L \tag{A-23}$$

Thus, the maximum interfacial shearing stress in a short enough assembly increases with an increase in the assembly length and is inversely proportional to the BGA stand-off height.

As to the interfacial peeling stress, it can be sought, in an approximate analysis, as

$$p(x) = K[w_1(x) - w_2(x)] \tag{A-24}$$

Here K is the spring constant of the BGA in the through-thickness direction. The relationship (A-24) reflects an assumption that the deflections of the PCB and the package have to be different in the given cross-section of the assembly to result in a non-zero peeling stress. By differentiation we find:

$$p''(x) = K[w_1''(x) - w_2''(x)], \qquad p'''(x) = K[w_1'''(x) - w_2'''(x)] \tag{A-25}$$

Since there are no concentrated bending moments, nor concentrated lateral forced at the assembly ends, the right parts of these equations should be zero at the ends, and therefore the following boundary conditions should be fulfilled for the sought peeling stress:

$$p''(\pm L) = 0, \ p'''(\pm L) = 0. \tag{A-26}$$

Introducing the formulas (A-8) into the first formula in (A-25) and differentiating the obtain expression twice with respect to the coordinate x, we obtain the following equation for the peeling stress function $p(x)$:

$$p^{IV}(x) + 4\beta^4 p(x) = -\mu K \frac{\Delta\alpha\Delta t}{\kappa} \frac{\cosh kx}{\cosh kL}, \tag{A-27}$$

where

$$\beta = \sqrt[4]{K \frac{D_1 + D_2}{4D_1 D}} \tag{A-28}$$

is the parameter of the peeling stress. Considering (A-28), the equation (A-27) can be written as follows:

$$p^{IV}(x) + 4\beta^4 p(x) = -4\beta^4 p_0 \frac{\cosh kx}{\cosh kL}, \tag{A-29}$$

where the notation

$$p_0 = \mu \frac{\Delta\alpha\Delta t}{\kappa} \frac{D_1 D_2}{D_1 + D_2} \tag{A-30}$$

is used. It is noteworthy that the equation (A-27) has the form of an equation of bending of beams supported by an elastic foundation.

We seek the solution to the equation (A-29) in the form:

$$p(x) = C_0 V_0(\beta x) + C_2 V_2(\beta x) - p_0 \frac{\eta^4}{1+\eta^4} \frac{\cosh kx}{\cosh kL}. \tag{A-31}$$

Here

$$\eta = \frac{\beta\sqrt{2}}{k} \tag{A-32}$$

is the ratio of the parameters of the peeling and the shearing stresses. The first two terms in the right part of the solution (A-31) represent the general solution to the homogeneous equation that corresponds to the equation (A-29) and the last term is the particular solution to the inhomogeneous equation (A-29). The functions $V_i(\beta x)$, $i = 0,1,2,3$, are as follows:

$$V_0(\beta x) = \cosh\beta x \cos\beta x, \quad V_2(\beta x) = \sinh\beta x \sin\beta x,$$

$$V_{1,3}(\beta x) = \frac{1}{\sqrt{2}}(\cosh\beta x \sin\beta x \pm \sinh\beta x \cos\beta x), \tag{A-33}$$

and obey the following rules of differentiation:

$$V_0'(\beta x) = -\beta\sqrt{2}V_3(\beta x), \ V_1'(\beta x) = \beta\sqrt{2}V_0(\beta x),$$

$$V_2'(\beta x) = \beta\sqrt{2}V_1(\beta x), \ V_3'(\beta x) = \beta\sqrt{2}V_2(\beta x). \tag{A-34}$$

Using the boundary conditions (A-26) we obtain the following equations for the constants C_0 and C_2 of integration

$$V_2(u)C_0 - V_0(u)C_2 = -\frac{\eta^2}{1+\eta^4} p_0,$$

$$V_1(u)C_0 + V_3(u)C_2 = -\frac{\eta}{1+\eta^4} p_0 \tanh kL, \tag{A-35}$$

where $u = \beta L$. The equations (A-35) yield:

$$C_0 = -2\sqrt{2}\frac{\eta}{1+\eta^4}p_0\frac{\eta V_3(u)+V_0(u)\tanh kL}{\sinh 2u+\sin 2u}$$
$$C_2 = -2\sqrt{2}\frac{\eta}{1+\eta^4}p_0\frac{-\eta V_1(u)+V_2(u)\tanh kL}{\sinh 2u+\sin 2u} \qquad \text{(A-36)}$$

and the solution (A-31) leads to the following expression for the peeling stress:

$$p(x) = -2\sqrt{2}\frac{\eta}{1+\eta^4}p_0\left[\frac{\eta V_3(u)+V_0(u)\tanh kL}{\sinh 2u+\sin 2u}V_0(\beta x)+\frac{-\eta V_1(u)+V_2(u)\tanh kL}{\sinh 2u+\sin 2u}V_2(\beta x)\right]-$$
$$-\frac{\eta^4}{1+\eta^4}p_0\frac{\cosh kx}{\cosh kL} \qquad \text{(A-30)}$$

For a long assembly $(kL \geq 2.5)$ this solution yields:

$$p(x) = -\frac{1}{4}\frac{\eta}{1+\eta^4}p_0 e^{-\beta(L-x)}\left[\eta(\sin(\beta(L-x)-\cos(\beta(L-x))+\sqrt{2}\cos(\beta(L-x)\right]-\frac{\eta^4}{1+\eta^4}p_0 e^{-k(L-x)} \qquad \text{(A-31)}$$

At the end $x = L$:

$$p(L) = -\frac{1}{4}p_0\frac{\eta}{1+\eta^4}\left(-\eta+\sqrt{2}+4\eta^3\right). \qquad \text{(A-32)}$$

For large ratios $\eta = \frac{\beta\sqrt{2}}{k}$ of the parameter of the peeling stress to the parameter of the shearing stress this formula leads to the following simple result: $p(L) = -p_0$. This result explains the physical meaning of the p_0 value: it is the peeling stress at the end of a long and stiff assembly. The formula (A-30) indicates that this stress is inversely proportional to the interfacial compliance κ and, hence, to the standoff height h of the BGA attachment. Thus, for long and stiff assemblies, the peeling stress is even more sensitive to the increase in the BGA standoff height than the interfacial shearing stress. The peeling stress is next to zero for short $(kL \leq 0.25)$ BGA attachments.